



Electronic structure of the 344-type superconductors $\text{La}_3(\text{Ni};\text{Pd})_4(\text{Si};\text{Ge})_4$ by *ab initio* calculations

M.J. Winiarski, M. Samsel-Czekala *

Institute of Low Temperature and Structure Research, Polish Academy of Sciences, P.O. Box 1410, 50-950 Wrocław 2, Poland

ARTICLE INFO

Article history:

Received 17 July 2012

Accepted 17 August 2012

Available online 25 August 2012

Keywords:

Superconductors

Intermetallics

Rare earth alloys and compounds

Transition metal alloys and compounds

Electronic band structure

Electron–phonon interactions

ABSTRACT

Electronic structures of superconducting ternaries: $\text{La}_3\text{Ni}_4\text{Si}_4$, $\text{La}_3\text{Ni}_4\text{Ge}_4$, $\text{La}_3\text{Pd}_4\text{Si}_4$, $\text{La}_3\text{Pd}_4\text{Ge}_4$, and their non-superconducting counterpart, $\text{La}_3\text{Rh}_4\text{Ge}_4$, have been calculated employing the full-potential local-orbital method within the density functional theory. Our investigations were focused particularly on densities of states (DOSs) at the Fermi level with respect to previous experimental heat capacity data, and Fermi surfaces (FSs) being very similar for all considered here compounds. In each of these systems, the FS originating from several bands contains both holelike and electronlike sheets possessing different dimensionality, in particular quasi-two-dimensional cylinders with nesting properties. A comparative analysis of the DOSs and FSs in these 344-type systems as well as in nickel (oxy)pnictide and borocarbide superconductors indicates rather similar phonon mechanism of their superconductivity.

© 2012 Elsevier B.V. All rights reserved.

1. Introduction

Intermetallics forming layered PbO-type structures have recently drawn wide interest since the discovery in 2008 of high-temperature (high- T_C) superconducting iron (oxy)pnictides reaching T_C up to 55 K [1]. However, isostructural with them nickel-based (oxy)pnictides do not exhibit such high T_C 's [2–4]. The pnictidlike structures are strongly anisotropic (quasi-two-dimensional, Q2D), being built from positively charged layers of atoms of alkaline or rare-earth metals and negatively charged layers containing transition metals and non-metallic atoms. The comparison of electronic structure between similar superconducting systems but based on various transition-metal elements may be crucial in understanding mechanisms of high- T_C SC in the iron-based class of these compounds and its lack in other ones.

Four superconductors: $\text{La}_3\text{Ni}_4\text{Si}_4$ ($T_C \sim 1.0$ K), $\text{La}_3\text{Ni}_4\text{Ge}_4$ ($T_C \sim 0.8$ K), $\text{La}_3\text{Pd}_4\text{Si}_4$ ($T_C \sim 2.2$ K), and $\text{La}_3\text{Pd}_4\text{Ge}_4$ ($T_C \sim 2.8$ K) have been reported [5–9] among orthorhombic 344-type systems. They adopt the $\text{U}_3\text{Ni}_4\text{Si}_4$ -type structure (*Immm*), resembling that of (oxy)pnictides, with a large ratio ($c/a \sim 6$). Among this kind of ternaries, non-superconducting representatives are $\text{La}_3\text{Rh}_4\text{Ge}_4$ [10], $\text{Ce}_3\text{Rh}_4\text{Ge}_4$, $\text{Ce}_3\text{Rh}_3\text{IrGe}_4$ [11] and Kondo-lattice $\text{Ce}_3\text{Pd}_4\text{Ge}_4$ [12] systems. On the other hand, lanthanides in the $\text{Ln}_3\text{Pd}_4\text{Ge}_4$ family ($\text{Ln} = \text{Y, Gd, Tb, Dy, Ho, Er, Tm}$ and Yb) [13–18] with other orthorhombic structure of the $\text{Gd}_3\text{Cu}_4\text{Ge}_4$ -type, forming Pd–Ge cages, exhibit no superconductivity (SC). A comparison between the structural

properties of the orthorhombic $\text{La}_3\text{Pd}_4\text{Ge}_4$ and tetragonal LaPd_2Ge_2 ($T_C \sim 1.1$ K) systems suggested that SC in this class of compounds is sensitive to an arrangement of transition-metal and non-metal atoms as in the Pd–Ge network [7].

In this work, we study electronic structure of the lanthanum 344-type family of superconductors: $\text{La}_3\text{Ni}_4\text{Si}_4$, $\text{La}_3\text{Ni}_4\text{Ge}_4$, $\text{La}_3\text{Pd}_4\text{Si}_4$, $\text{La}_3\text{Pd}_4\text{Ge}_4$, and their non-superconducting reference compound, $\text{La}_3\text{Rh}_4\text{Ge}_4$, by *ab initio* methods. Our investigations are focused on a relation between their densities of states (DOSs) at the Fermi level (E_F) and T_C values. Also their Fermi surfaces (FSs) topology is compared with that of $\text{La}_3\text{Rh}_4\text{Ge}_4$. Furthermore, we discuss their electronic structure similarities to those of (oxy)pnictide and borocarbide superconductors.

2. Computational methods

Electronic structure of all considered here 344-type compounds, crystallizing in the orthorhombic *Immm* structure (visualized in Fig. 1), have been computed with the full-potential local-orbital (FPLO-9) method [19]. The Perdew–Wang form [20] of the local density approximation (LDA) of exchange–correlation functional was employed in the scalar relativistic mode.

X-ray diffraction values of lattice parameters (in nm) used in our calculations, taken from Ref. [7], are as follows: $a = 0.41305$, $b = 0.41760$, $c = 2.3578$ for $\text{La}_3\text{Ni}_4\text{Si}_4$; $a = 0.42017$, $b = 0.42167$, $c = 2.4031$ for $\text{La}_3\text{Ni}_4\text{Ge}_4$; $a = 0.42254$, $b = 0.43871$, $c = 2.4551$ for $\text{La}_3\text{Pd}_4\text{Si}_4$; $a = 0.42293$, $b = 0.43823$, $c = 2.50109$ for $\text{La}_3\text{Pd}_4\text{Ge}_4$; $a = 0.41746$, $b = 0.42412$, $c = 2.5234$ for $\text{La}_3\text{Rh}_4\text{Ge}_4$. The experimental atomic positions, given in [7], were assumed as initial ones and then optimized for all investigated compounds to minimize forces in the unit cell (u.c.), containing double formula unit (f.u.), prior to further band structure computations. Valence-basis sets were automatically selected by the FPLO-9 internal procedure. Total energy values

* Corresponding author. Tel.: +48 71 3954 322; fax: +48 71 344 10 29.

E-mail address: m.samsel@int.pan.wroc.pl (M. Samsel-Czekala).

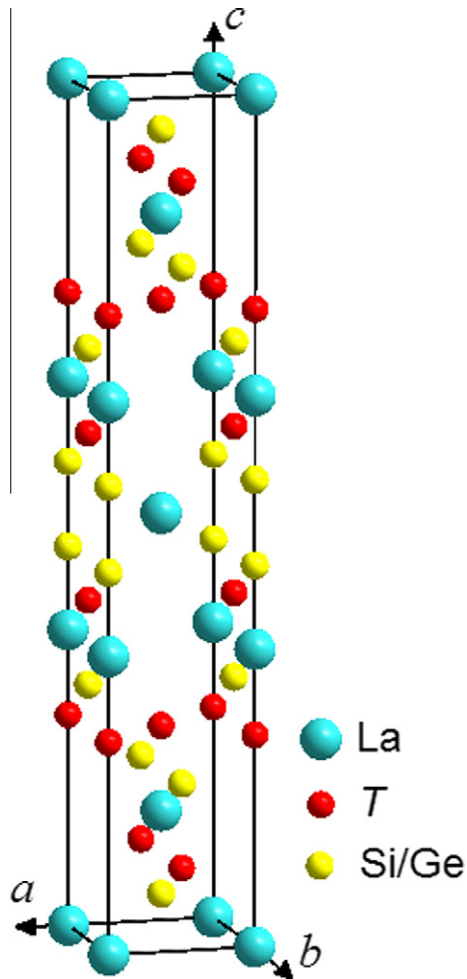


Fig. 1. Unit cell of $\text{La}_3\text{T}_4(\text{Si/Ge})_4$ systems ($T = \text{Ni, Pd, Rh}$) of the $\text{U}_3\text{Ni}_4\text{Si}_4$ -type ($I4mmm$, No. 71).

of the considered here systems were converged with accuracy to ~ 1 meV for the $16 \times 16 \times 16$ k -point mesh, yielding 621 k -points in the irreducible part of the Brillouin zone (BZ).

3. Results and discussion

The total and partial DOSs of five probed here systems are plotted in Fig. 2. Their overall shapes, being similar to one another, are dominated by the broad peaks of the transition-metal (Ni, Pd, Rh) 3d/4d and non-metal (Si, Ge) 3p/4p, as well as La 5d electron orbitals. The highest peaks of the Ni 3d and Rh 4d electrons are centered at about 1.5–2.0 eV below the Fermi level while those coming from a greater number of Pd 4d electrons are located deeper in energy, i.e. 3.0–3.5 eV below E_F . Hence, they have slightly smaller contributions at E_F than those of the Ni-based systems. For the considered here ternaries, the total DOSs at E_F , $N(E_F)$, are collected in Table 1. It presents both our calculated (LDA) and experimental $N(E_F)$, derived from heat capacity data of Ref. [9]. This table indicates that the LDA values of $N(E_F)$ are all slightly smaller than the corresponding experimental data. Nevertheless, both theoretical and experimental $N(E_F)$ are inversely proportional to the superconducting transition temperatures, T_C 's. This fact can be explained by the strong influence of the electron–phonon coupling on SC in this family of compounds as postulated in Ref. [9].

As is visible in Fig. 2, in $\text{La}_3\text{Ni}_4(\text{Si/Ge})_4$ the Fermi level is placed near the narrow sub-peak originating mainly from the Ni 3d electrons, which resembles the situation taking place in other nickel-

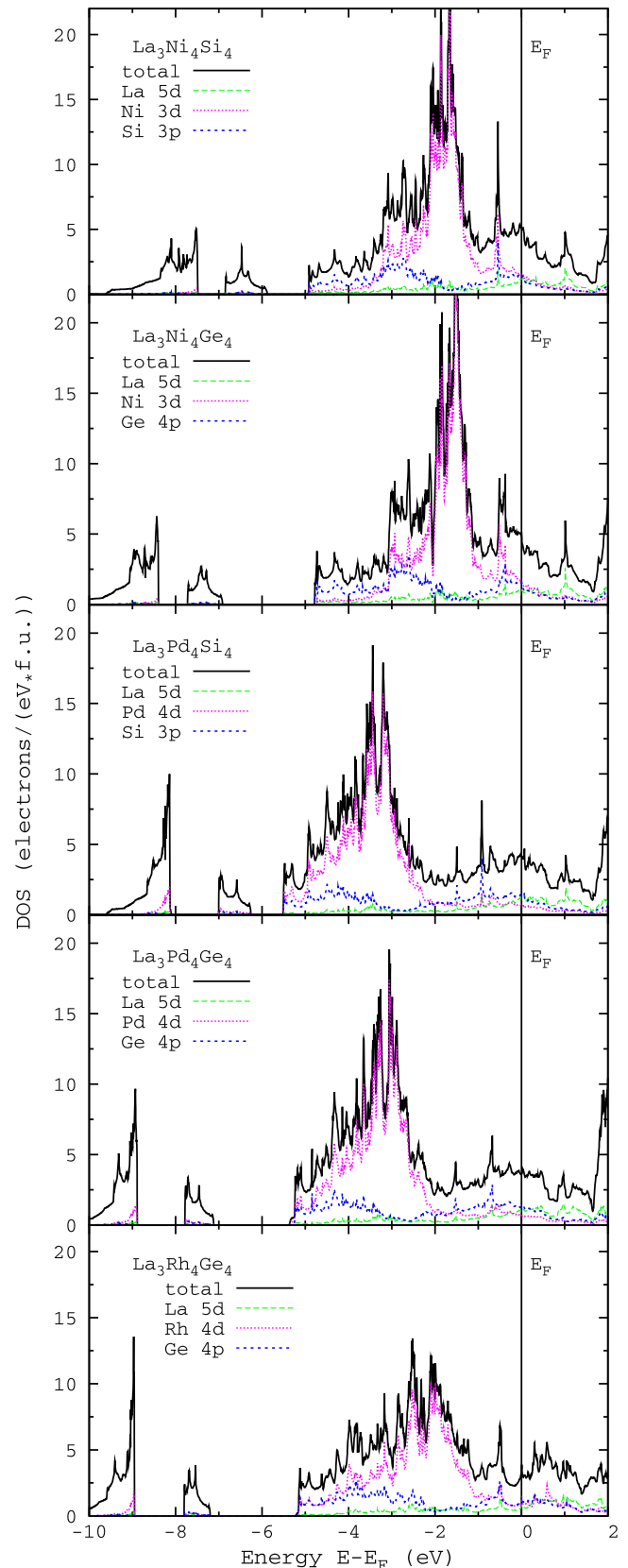


Fig. 2. Calculated (LDA) total and partial (per electron orbitals of transition-metal, 3d/4d/5d, and other, 3p/4p, atoms) DOSs in $\text{La}_3\text{T}_4\text{X}_4$ for $T = \text{Ni, Pd, Rh}$ and $X = \text{Si, Ge}$.

based systems possessing the $I4/mmm$ symmetry [21,22]. It enables further T_C tuning by any change in DOS at E_F , in analogy to

Table 1

Our computed (LDA) total DOSs at E_F , $N(E_F)$ (in electrons/eV/f.u.) and available experimental values of $N(E_F)$ and maximum T_C 's (in K), for the $\text{La}_3(\text{Ni};\text{Pd})_4(\text{Si};\text{Ge})_4$ ternaries [5–9].

Compound	Calculated $N(E_F)$	Experimental $N(E_F)$	Maximum T_C
$\text{La}_3\text{Ni}_4\text{Si}_4$	5.1	5.3–5.4 [9]	1.0 [8,9]
$\text{La}_3\text{Ni}_4\text{Ge}_4$	5.0	5.0–5.2 [9]	0.8 [9]
$\text{La}_3\text{Pd}_4\text{Si}_4$	4.2	–	2.2 [6]
$\text{La}_3\text{Pd}_4\text{Ge}_4$	3.6	3.7–3.9 [9]	2.8 [5,7]
$\text{La}_3\text{Rh}_4\text{Ge}_4$	3.4	–	–

the borocarbides [23], where the Fermi level is situated exactly at the local maximum of DOSs. For the stronger electron–phonon coupled palladium-based systems [9], their DOS's in the vicinity of E_F are diminished and become quite flat. In consequence, one may expect rather insignificant pressure effects on the electronic structure and related properties of this series.

Our calculated electronic occupation numbers, N_{calc} , in the investigated here 344-type compounds, compared with those for the free atoms, N_{at} , are given in Table 2. The electron populations for La, Si and Ge orbitals are similar in all considered here systems. Namely, for La 5d electrons $N_{\text{calc}} = 1.4$, being enhanced compared with $N_{\text{at}} = 1$. This is in contrary to strongly reduced N_{calc} (~ 0.2) of the La 6s electrons with respect to its $N_{\text{at}} (=2)$. In turn, N_{calc} 's for both the Si 3s and Ge 4s electrons have slightly diminished N_{calc} (~ 1.5) in relation to their $N_{\text{at}} (=2)$. Whereas N_{calc} 's for the Si 3p and Ge 4p electrons are substantially higher (~ 3.0) than $N_{\text{at}} (=2)$. Interestingly, in both Ni-based superconductors, the Ni 3d electrons have $N_{\text{calc}} = 8.8$, being strongly enhanced with respect to $N_{\text{at}} = 8$. This is opposite behavior to that of the Pd-based superconductors, where the Pd 4d electrons possess much reduced N_{calc} (~ 9.0) compared with $N_{\text{at}} (=10)$. Meanwhile, in the case of the non-superconducting compound with rhodium, for the Rh 4d electrons, $N_{\text{calc}} \sim 8.3$ is only slightly increased ($N_{\text{at}} = 8$). Finally, Ni/Pd/Rh 4s/5s and 4p/5p electrons have similar $N_{\text{calc}} \sim 0.5$, though they have different values of N_{at} .

The calculated bands energies, are plotted in Fig. 3 only for two chosen superconductors, i.e. $\text{La}_3\text{Ni}_4\text{Si}_4$ and $\text{La}_3\text{Pd}_4\text{Ge}_4$, and also for the reference compound, $\text{La}_3\text{Rh}_4\text{Ge}_4$. As this figure indicates, the band structures of both mentioned above superconductors as well as of the other ones (not displayed here), considered in this paper, are quite similar to one another at E_F , compared with a reduced number of bands cutting E_F in the non-superconducting $\text{La}_3\text{Rh}_4\text{Ge}_4$. It is also seen in Fig. 3 that the band structure in these superconductors could be the most sensitive to pressure or doping along the ΓX and XU1 lines.

The Fermi surfaces of the considered above three compounds, i.e. $\text{La}_3\text{Ni}_4\text{Si}_4$, $\text{La}_3\text{Pd}_4\text{Ge}_4$ and $\text{La}_3\text{Rh}_4\text{Ge}_4$, are displayed in Fig. 4. As is visible in this figure, the FSs are quite similar for the nickel- and palladium-based superconductors, originating from as many as six bands, while in the reference rhodium-based system its FS comes from only five bands. All FSs contain three-dimensional (3D) holelike pockets and complex sheets of I and II conduction bands. In turn, the electronlike FS sheets in III–VI bands form

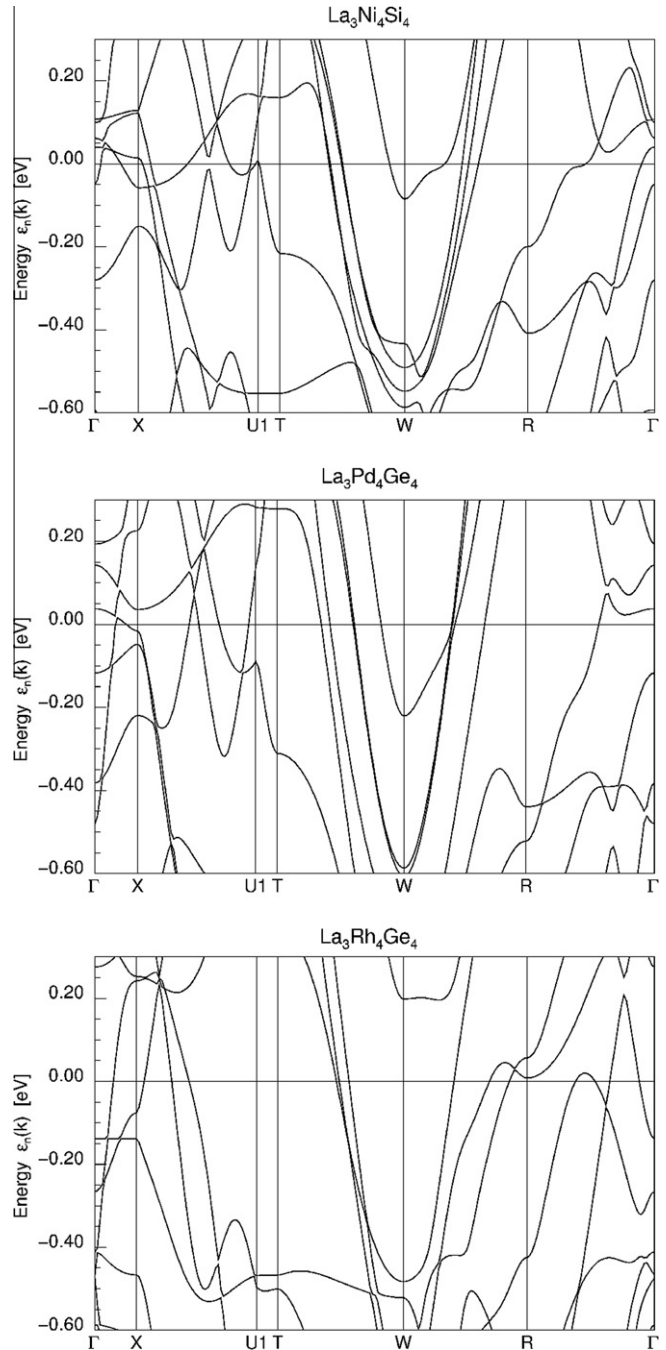


Fig. 3. Computed (LDA) band structures of two chosen superconductors, $\text{La}_3\text{Ni}_4\text{Si}_4$ and $\text{La}_3\text{Pd}_4\text{Ge}_4$, compared with that of non-superconducting $\text{La}_3\text{Rh}_4\text{Ge}_4$, displayed in the vicinity of E_F .

Q2D corrugated cylinders, centered at the S points, being also characteristic of other pnictidlike superconductors [21,22,24]. Such

Table 2

Calculated (LDA) electron occupation numbers, N_{calc} , (per given orbital at single atomic position) for $\text{La}_3\text{T}_4(\text{Si};\text{Ge})_4$ systems (with accuracy to ± 0.1), compared with the corresponding numbers for free atoms, N_{at} (given in parentheses). It should be noticed that in each system, N_{calc} of the same electron orbitals in T and Si/Ge atoms are varying (± 0.4) depending on their atomic positions in the u.c., from which given orbitals originate.

Compound	La 5d	La 6s	T 3d/4d	T 4s/5s	T 4p/5p	Si 3s/Ge 4s	Si 3p/Ge 4p	Si 3d/Ge 4d
$\text{La}_3\text{Ni}_4\text{Si}_4$	1.4 (1)	0.2 (2)	Ni 3d 8.8 (8)	Ni 4s 0.6–0.8 (2)	Ni 4p 0.5 (0)	1.4–1.5 (2)	2.8–2.9 (2)	0.3 (0)
$\text{La}_3\text{Ni}_4\text{Ge}_4$						1.5–1.6 (2)	2.8–3.2 (2)	0.1 (0)
$\text{La}_3\text{Pd}_4\text{Si}_4$			Pd 4d 9.0 (10)	Pd 5s 0.6–0.7 (0)	Pd 5p 0.5 (0)	1.5 (2)	2.8–3.0 (2)	0.2–0.3 (0)
$\text{La}_3\text{Pd}_4\text{Ge}_4$			Pd 4d 9.0–9.1 (10)		Pd 5p 0.4 (0)	1.6 (2)	2.9–3.2 (2)	0.1–0.2 (0)
$\text{La}_3\text{Rh}_4\text{Ge}_4$			Rh 4d 8.2–8.4 (8)	Rh 5s 0.5–0.6 (1)	Rh 5p 0.3 (0)	1.6–1.7 (2)	2.9–3.1 (2)	

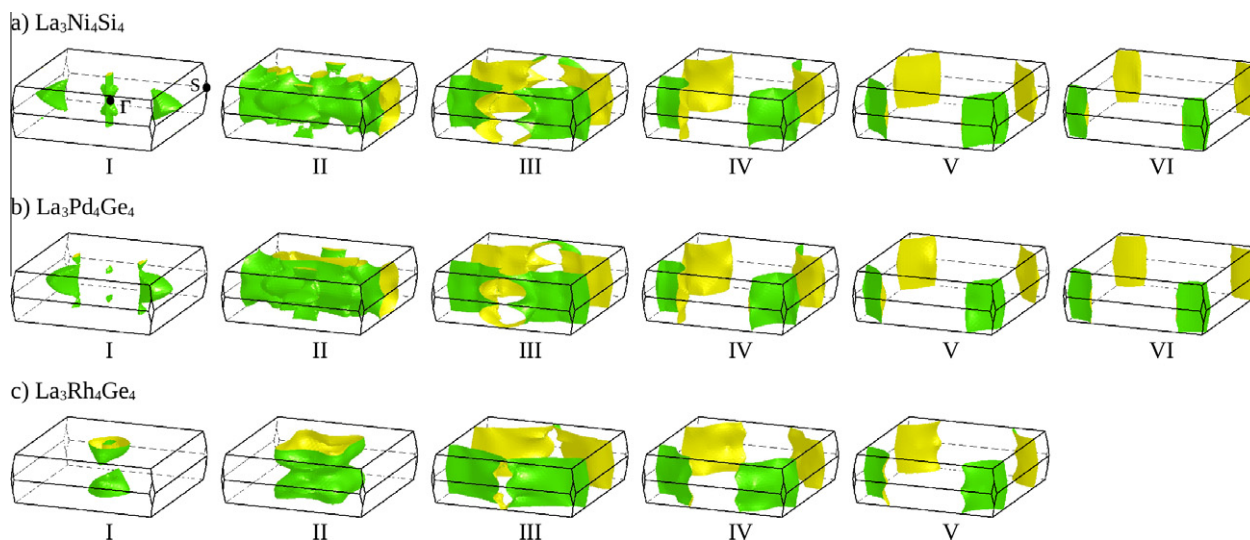


Fig. 4. Calculated (LDA) FS sheets originating from a few bands (denoted as I–VI), drawn separately within the orthorhombic $Immm$ -type BZ boundaries, for superconductors: (a) $\text{La}_3\text{Ni}_4\text{Si}_4$ and (b) $\text{La}_3\text{Pd}_4\text{Ge}_4$, as well as (c) non-superconducting $\text{La}_3\text{Rh}_4\text{Ge}_4$. The FS sheets I–II reveal holelike and III–VI – electronlike characters.

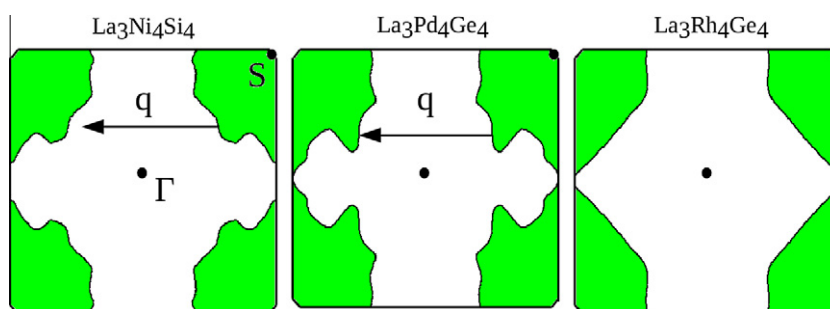


Fig. 5. Calculated sections of III FS sheets (shown in Fig. 4) through the basal (001) plane, for two superconductors, $\text{La}_3\text{Ni}_4\text{Si}_4$ and $\text{La}_3\text{Pd}_4\text{Ge}_4$, and non-superconducting $\text{La}_3\text{Rh}_4\text{Ge}_4$. The arrow denotes nesting vector $\mathbf{q} = 0.5 \times (2\pi/\mathbf{b})$, being suitable for spanning electron surfaces of the Pd-based superconductors. Green color marks area occupied by electrons.

complex FSs allow for multi-band SC, particularly as in the case of borocarbides [23,24]. It also turned out that in the nickel-borocarbide $\text{LuNi}_2\text{B}_2\text{C}$ superconductor, specific nesting features in electronlike FS sheets can be responsible for strong Kohn (electron-phonon) anomalies, enhancing rather BCS-like SC [24]. It should be underlined here that only for the palladium-based superconductors, we have obtained, in our LDA calculations, an analogous perfect nesting with the vector $\mathbf{q} = 0.5 \times (2\pi/\mathbf{b})$, which is drawn in Fig. 5. It is also seen in this figure that such a nesting is much less perfect in the case of the nickel-based superconductors but completely lacking in the non-superconducting $\text{La}_3\text{Rh}_4\text{Ge}_4$ system. This nesting feature might explain an enhancement of T_C for the palladium-based superconductors as connected with possible electron-phonon anomalies, which requires additional experimental studies.

4. Conclusions

The band structures of four superconductors $\text{La}_3(\text{Ni;Pd})_4(\text{Si;Ge})_4$ and the non-superconducting reference system, $\text{La}_3\text{Rh}_4\text{Ge}_4$, have been studied from the first principles. Our calculated densities of states at the Fermi level are inversely proportional to the T_C 's, which supports the assumption, derived from previous experimental data, that superconductivity in this class of compounds can be strongly driven by the strength of the electron-phonon coupling.

Therefore, as expected, higher T_C are reached by systems with lower DOSs at E_F . The multi-band Fermi surfaces of all investigated here superconductors, allowing for an occurrence of multi-gap superconductivity, are similar to one another. The FSs originate from six bands and contain three-dimensional holelike pockets and complex sheets as well as quasi-two-dimensional corrugated electronlike cylinders. The nesting properties of electron III FS sheet of $\text{La}_3\text{Pd}_4\text{Ge}_4$ indicates that superconductivity for palladium-based compounds may be additionally enhanced due to electron-phonon anomalies, as it happens in the case of nickel borocarbide superconductors.

Acknowledgments

The National Center for Science in Poland is acknowledged for financial support of Project No. N N202 239540. The calculations were carried out mainly in Wrocław Center for Networking and Supercomputing (Project No. 158). The Computing Center at the Institute of Low Temperature and Structure Research PAS in Wrocław is also acknowledged for the use of the supercomputers and technical support.

References

- [1] R.H. Liu, G. Wu, T. Wu, D.F. Fang, H. Chen, S.Y. Li, K. Liu, Y.L. Xie, X.F. Wang, R.L. Yang, L. Ding, C. He, D.L. Feng, X.H. Chen, Phys. Rev. Lett. 101 (2008) 087001;

- G. Wu, Y.L. Xie, H. Chen, M. Zhong, R.H. Liu, B.C. Shi, Q.J. Li, X.F. Wang, T. Wu, Y.J. Yan, J.J. Ying, X.H. Chen, *J. Phys.: Condens. Matter* 21 (2009) 142203.
- [2] T. Watanabe, H. Yanagi, Y. Kamihara, T. Kamiya, M. Hirano, H. Hosono, *J. Solid State Chem.* 181 (2008) 2117;
T. Watanabe, H. Yanagi, T. Kamiya, Y. Kamihara, H. Hiramoto, M. Hirano, H. Hosono, *Inorg. Chem.* 46 (2007) 7719;
W.-B. Zhang, X.-B. Xiao, W.-Y. Yu, N. Wang, B.-Y. Tang, *Phys. Rev. B* 77 (2008) 214513.
- [3] T. Mine, H. Yanagi, T. Kamiya, Y. Kamihara, M. Hirano, H. Hosono, *Solid State Commun.* 147 (2008) 111.
- [4] F. Ronning, E.D. Bauer, T. Park, N. Kurita, T. Klimczuk, R. Movshovich, A.S. Sefat, D. Mandrus, J.D. Thompson, *Physica C* 469 (2009) 396;
A. Subedi, D.J. Singh, *Phys. Rev. B* 78 (2008) 132511.
- [5] H. Fujii, T. Mochiku, H. Takeya, A. Sato, *Phys. Rev. B* 72 (2005) 214520.
- [6] H. Fujii, *J. Phys.: Condens. Matter* 18 (2006) 8037.
- [7] T. Mochiku, H. Fujii, H. Takeya, T. Wuernisha, T. Ishigaki, T. Kamiyama, K. Hirata, K. Mori, *Physica C* 463–465 (2007) 182.
- [8] H. Fujii, S. Kasahara, *J. Phys.: Condens. Matter* 20 (2008) 075202.
- [9] S. Kasahara, H. Fujii, H. Takeya, T. Mochiku, A.D. Thakur, K. Hirata, *J. Phys.: Condens. Matter* 20 (2008) 385204.
- [10] T. Ohta, F. Izumi, K. Oikawa, T. Kamiyama, *Physica B* 234 (1997) 1093.
- [11] P. Rogl, B. Chevalier, J. Etourneau, *J. Solid State Chem.* 88 (1990) 429.
- [12] H.I. Im, Y.S. Kwon, M.H. Jung, *Solid State Commun.* 124 (2002) 181.
- [13] W. Rieger, *Monatsch. Chem.* 101 (1970) 449.
- [14] O. Liebrich, H. Schafer, A. Weiss, *Z. Naturforsch. B* 25 (1970) 650.
- [15] R.E. Gladyshevskii, O.L. Sologub, E. Parthe, *J. Alloy. Compd.* 176 (1991) 329.
- [16] Yu.M. Prots, O.I. Bodak, V.K. Pecharsky, P.S. Salamakha, Yu.D. Seropegin, *Z. Kristallogr.* 205 (1993) 331.
- [17] P. Salamakha, O. Sologub, J.K. Yakinthos, Ch.D. Routsis, *J. Alloy. Compd.* 267 (1998) 192.
- [18] D. Niepmann, Y.M. Prots, R. Pottgen, W. Jeitschko, *J. Solid State Chem.* 154 (2000) 329.
- [19] FPLO9.00-34, improved version of the FPLO code by K. Koepnik, H. Eschrig, *Phys. Rev. B* 59 (1999) 1743.
- [20] J.P. Perdew, Y. Wang, *Phys. Rev. B* 45 (1992) 13244.
- [21] I.R. Shein, A.L. Ivanovskii, *Phys. Rev. B* 79 (2009) 054510.
- [22] I.R. Shein, A.L. Ivanovskii, *JETP Lett.* 89 (2009) 285.
- [23] W.E. Pickett, D.J. Singh, *Phys. Rev. Lett.* 72 (1994) 3702;
P. Dervegas, M. Bullock, J. Zarestky, P. Canfield, B.K. Cho, B. Harmon, A.I. Goldman, C. Stassis, *Phys. Rev. B* 52 (1995) R9839;
B. Bergk, V. Petzold, H. Rosner, S.-L. Drechsler, M. Bartkowiak, O. Ignatchik, A.D. Bianchi, I. Sheikin, P.C. Canfield, J. Wosnitza, *Phys. Rev. Lett.* 100 (2008) 257004;
T. Terashima, C. Haworth, H. Takeya, S. Uji, H. Aoki, K. Kadowaki, *Phys. Rev. B* 56 (1997) 5120;
K. Yamauchi, H. Katayama-Yoshida, A. Yanase, H. Harima, *Physica C* 412–414 (2004) 225.
- [24] S.B. Dugdale, M.A. Alam, I. Wilkinson, R.J. Hughes, I.R. Fisher, P.C. Canfield, T. Jarlborg, G. Santi, *Phys. Rev. Lett.* 83 (1999) 4824.